

## A Light-Activated Reaction Manifold

Kai Hildebrandt,<sup>†,‡</sup> Katharina Elies,<sup>†</sup> Dagmar R. D'hooge,<sup>§,||</sup> James P. Blinco,<sup>\*,⊥</sup>  
and Christopher Barner-Kowollik<sup>\*,†,‡,⊥</sup>

<sup>†</sup>Preparative Macromolecular Chemistry, Institut für Technische Chemie und Polymerchemie, Karlsruhe Institute of Technology (KIT), Engesserstraße 18, 76128 Karlsruhe, Germany

<sup>‡</sup>Institut für Biologische Grenzflächen (IBG), Karlsruhe Institute of Technology (KIT), Hermann-von-Helmholtz-Platz 1, 76344 Eggenstein-Leopoldshafen, Germany

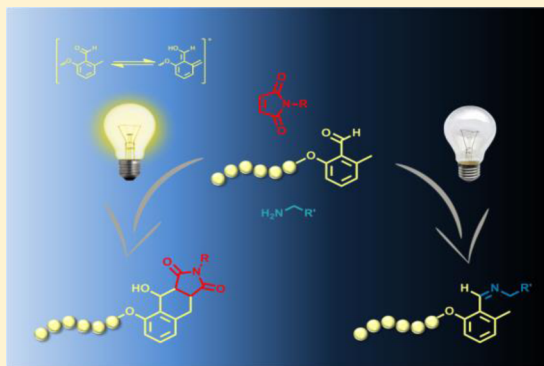
<sup>§</sup>Department of Chemical Engineering and Technical Chemistry, Laboratory for Chemical Technology, Ghent University, Technologiepark 914, B-9052 Gent, Belgium

<sup>||</sup>Department of Textiles, Ghent University, Technologiepark 907, B-9052 Gent, Belgium

<sup>⊥</sup>School of Chemistry, Physics and Mechanical Engineering, Queensland University of Technology (QUT), 2 George Street, Brisbane, QLD 4000, Australia

### Supporting Information

**ABSTRACT:** We introduce an efficient reaction manifold where the rate of a thermally induced ligation can be controlled by a photonic field via two competing reaction channels. The effectiveness of the reaction manifold is evidenced by following the transformations of macromolecular chain termini via high-resolution mass spectrometry and subsequently by selective block copolymer formation. The light-controlled reaction manifold consists of a so-called *o*-quinodimethane species, a photocaged diene, that reacts in the presence of light with suitable enes in a Diels–Alder reaction and undergoes a transformation into imines with amines in the absence of light. The chemical selectivity of the manifold is controlled by the amount of ene present in the reaction and can be adjusted from 100% imine formation (0% photo product) to 5% imine formation (95% photo product). The reported light-controlled reaction manifold is highly attractive because a simple external field is used to switch the selectivity of specific reaction channels.



## INTRODUCTION

Orthogonal reactions are of high importance in all fields of chemistry, specifically to allow for bioorthogonality.<sup>1,2</sup> Ideally, the construction of a complex target molecule occurs in one pot via independently progressing, quantitative transformations.<sup>3,4</sup> There exist advanced approaches that use various click reactions in order to functionalize macromolecules,<sup>5</sup> synthesize dendrimers,<sup>6,7</sup> or pattern 3D cell environments.<sup>8,9</sup> Nevertheless, thermally induced click reactions lack spatial and temporal control, whereas photochemical approaches are able to overcome these disadvantages.<sup>10</sup> Most commonly, the spatial control of light-driven systems is exploited.<sup>11–13</sup> Although temporal control is often employed in photocuring systems<sup>14</sup> and pulsed laser polymerization,<sup>15</sup> this aspect has never been exploited for the generation of a reaction manifold between thermal and light-induced processes. *o*-Quinodimethanes (the photoenol product of *o*-methyl benzaldehydes) have been extensively reported to undergo a phototriggered [4 + 2]-cycloaddition with electron-poor enes such as maleimides,<sup>16</sup> dithioesters,<sup>17</sup> and even diphenylcarbenes.<sup>18</sup> The photoenolization–cycloaddition ligation is classified as a light-induced click reaction.<sup>19</sup> The reactivity

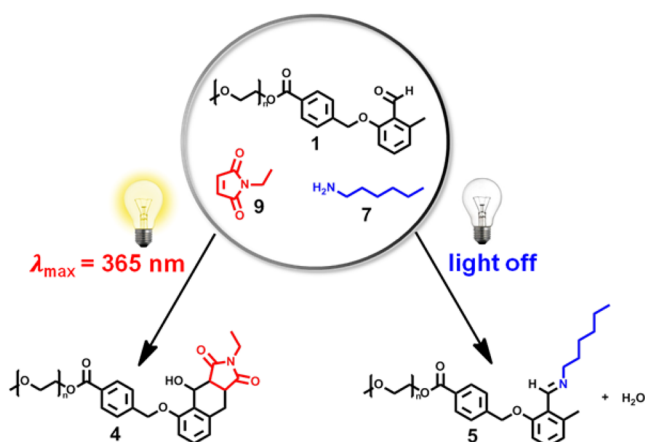
of the precursor benzaldehydes is based on the light-triggered isomerization of an *o*-methyl-substituted aromatic aldehyde into an *o*-quinodimethane species carrying a highly reactive diene functionality.<sup>20–22</sup> Reactions featuring *o*-quinodimethane moieties have been widely implemented into various areas including block copolymer synthesis,<sup>23</sup> the formation of cyclic polymers,<sup>24</sup> the modification of nanoparticles,<sup>25</sup> surface patterning procedures,<sup>26,19</sup> and the design of 3D micro scaffolds.<sup>27</sup> A wavelength selective manifold ( $\lambda$ -orthogonal ligation) has recently been introduced by us based on *o*-methyl benzaldehyde and nitrile imine driven chemistry.<sup>28</sup> Herein, we introduce a reaction manifold based on photoenolization–cycloaddition chemistry that can be simply switched to a preferred reaction pathway by switching a photonic field on or off (refer to Scheme 1).

## RESULTS AND DISCUSSION

The system rests on the ability of an aryl aldehyde (prior to photoenolisation) reacting with amines to yield a stable imine.

Received: February 24, 2016

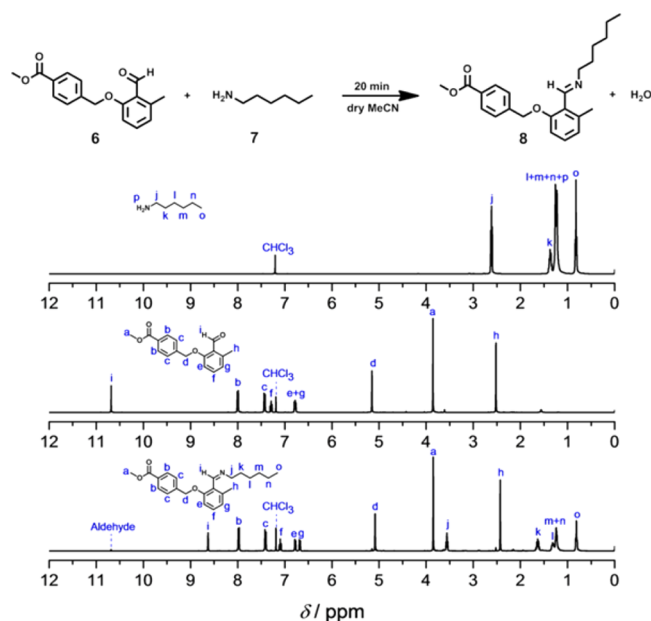
Published: May 6, 2016

Scheme 1. Selectivity of the Light-Controlled Reaction Manifold<sup>a</sup>

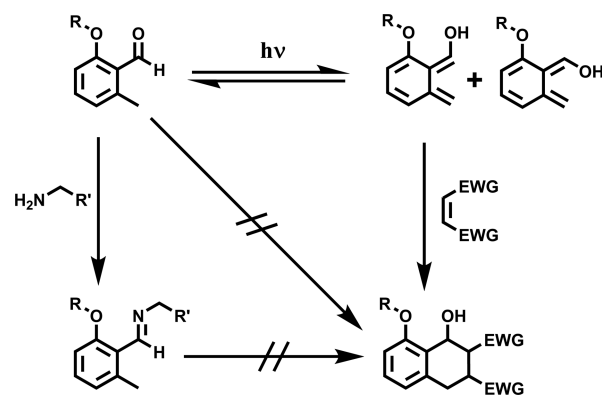
<sup>a</sup>The one-pot system consists of the photoactive *o*-methyl benzaldehyde terminated poly(ethylene glycol) (PEG,  $M_n = 2200 \text{ g mol}^{-1}$ ) 1, ethyl maleimide 9, and hexylamine 7. During irradiation, a photoinduced reaction between *o*-quinodimethane and maleimide predominantly takes place (left). Non-irradiation leads to exclusive imine formation (right).

However, when exposed to light activation the aryl aldehyde is readily transformed into a diene (*o*-quinodimethane or photoenol), which undergoes a Diels–Alder reaction with a maleimide and in its diene form is no longer able to undergo a thermal reaction with amines. A detailed description of the reaction mechanism and the kinetics of the manifold is provided below. The imine formation is a second-order catalyst-free reaction and fulfills certain click criteria including quantitative yield and no necessity for purifying the obtained product.<sup>29–31</sup> The versatility of the imine formation based on a benzaldehyde is demonstrated in a <sup>1</sup>H NMR study employing small molecules. An equimolar mixture of hexylamine 7 is stirred with methyl 4-((2-formyl-3-methylphenoxy)methyl)benzoate 6 in dry acetonitrile at ambient temperature. The imine formation can be traced by the aldehyde signal (peak i, Figure 1), which is shifted from 10.69 to 8.63 ppm. Concomitantly, the aryl methyl resonance (peak h, Figure 1) is shifted from 2.52 to 2.43 ppm. After 20 min, the yield of the imine is quantitative.

Because the thermal reaction path to the imine formation proceeds exclusively without irradiation there are in principle two possibilities how to generate selectivity while irradiating (Scheme 2): (i) Selectivity is accomplished through a simple rate difference. The photoreaction is intrinsically much faster than the thermal process, so it dominantly converts all *o*-methyl benzaldehyde species during irradiation, depleting the benzaldehyde concentration available for the thermal reaction. Essentially, however, the rate of the thermal reaction is not affected. (ii) Both intrinsic reactivities are similar or differ only slightly, and selectivity is introduced by transforming the *o*-methyl benzaldehyde into a species that is not reactive toward the amine via an equilibrium process, thus effectively decreasing the concentration of the aldehyde available for reaction with the amine. It is the latter process we will initially exploit and that carries the term “reaction manifold”. The light-triggered cycloaddition of a *o*-quinodimethane with electron-poor enes depends on the physical parameters of the irradiation source such as the wavelength range. In addition, the polarity of the solvent has a major influence on the benzaldehyde consumption



**Figure 1.** <sup>1</sup>H NMR study of the imine formation using methyl 4-((2-formyl-3-methylphenoxy)methyl)benzoate 6 (1.0 equiv) and hexylamine 7 (1.1 equiv) in CDCl<sub>3</sub>. A shift of the aryl methyl resonance (h) and the aldehyde resonance (i) of the benzaldehyde species toward higher fields is displayed.

Scheme 2. Light-Induced Equilibrium between the *o*-Methyl-Substituted Benzaldehyde and the *o*-Quinodimethane (Diene) Form<sup>a</sup>

<sup>a</sup>This equilibrium can be shifted towards the latter because of the presence of enes such as maleimides during irradiation. The electron poor ene acts as a diene trap for the *Z* isomer of the substituted *o*-quinodimethane, whereas the substituted *E* isomer is rapidly reverted to the aldehyde form, leading to the fast and continuous light-induced reformation of both diene forms. Therefore, the imine formation based on the benzaldehyde is strongly suppressed.

rate.<sup>32,33</sup> In polar solvents such as acetonitrile, the reaction is accelerated in comparison to that in nonprotic solvents such as dichloromethane. Initial kinetic studies of the photoreaction in acetonitrile and dichloromethane (no amine present) were performed in the presence of ethyl maleimide at fixed initial concentration (refer to Figure S14) to identify the solvent in which the rate of reaction is closest to that of the solvent-independent *o*-methyl benzaldehyde/amine conversion (refer to Figure S18). The photoenol in hydrogen-bonding solvents such as acetonitrile is more stabilized than that in dichloromethane, leading to a more efficient Diels–Alder reaction<sup>31</sup> (refer to Table

1). Thus, dichloromethane was selected as solvent to understand the principle ability of the reaction manifold.

**Table 1. Comparison of the Initial Benzaldehyde Consumption Rates in Acetonitrile and Dichloromethane under Irradiation (No Amine Present)<sup>a</sup>**

solvent	initial rate ( $10^{-4} \text{ L}\cdot\text{mol}^{-1}\cdot\text{s}^{-1}$ )
acetonitrile	9.0
dichloromethane	4.0

<sup>a</sup>These data showcase the initial choice of dichloromethane to study the working principle of the reaction manifold because it still facilitates imine formation.

**Evidencing the Reaction Manifold.** The one-pot system containing 1.0 equiv of benzaldehyde-capped poly(ethylene glycol) **1**, 1.2 equiv of ethyl maleimide **9**, and 3.6 equiv of hexylamine **7** in dry dichloromethane was implemented as a switchable reaction manifold. The dark time reaction proceeds at ambient temperature, leading to the exclusive transformation of the *o*-methyl substituted aromatic aldehyde with hexylamine into an imine moiety. The light-driven path induces the Diels–Alder reaction of the *o*-methyl benzaldehyde with ethyl maleimide into a [4 + 2] cycloadduct. We follow the conversion of the benzaldehyde species ( $1\cdot 10^{-3} \text{ mol}\cdot\text{L}^{-1}$ ) via quantitative high-resolution mass spectrometry.<sup>34</sup> Irradiation at  $\lambda_{\text{max}} = 365 \text{ nm}$  (refer to Figure S1 for the emission spectrum of the employed lamp) leads to quantitative benzaldehyde conversion to the Diels–Alder cycloadduct after 7 min (refer to Figure S13). During the same time, under identical conditions yet without irradiation, no conversion to the cycloadduct is observed, but conversion to the imine is found to be 23%. Scheme 2 summarizes the reactions defining the reaction manifold.

The benzaldehyde species can be transformed into the *E/Z* mixture of the *o*-quinodimethane species carrying a diene functionality via the irradiation process.<sup>35</sup> Hereby, the *Z* form is quickly reverted to the benzaldehyde (refer to Scheme 2). The *E*

form of the *o*-quinodimethane is solely able to undergo an irreversible cycloaddition with an ene carrying electron-withdrawing groups during irradiation.<sup>36</sup> The relative amount of the diene species decreases immediately, and as long as the irradiation proceeds, the equilibrium between the aldehyde and the diene shifts toward the diene according to Le Châtelier's principle (refer to Scheme 2).<sup>37,38</sup> To illustrate the principle ability of the reaction manifold to function, we carried out semiquantitative kinetic simulations using the PREDICI program package. The four reactions are depicted on the left-hand side of Figure 2 alongside their associated rate coefficients that were assessed on the basis of literature data and analysis of the composition of the system after predefined time intervals via high-resolution Orbitrap ESI-MS and <sup>1</sup>H NMR. Furthermore, we show that the initial amount of maleimide present in the reaction system governs the efficacy of the reaction manifold as expected by a fundamental reaction kinetic analysis (refer to the Supporting Information). The optimized deactivation rate coefficient of the photoenol ( $k_{\text{deact}} = 5.0 \times 10^{-1} \text{ s}^{-1}$ ) implies an average lifetime of 2 s, which is of a similar order of magnitude compared to the value of several seconds, as previously assessed.<sup>35</sup> The light-triggered activation rate coefficient of the benzaldehyde species,  $k_{\text{act}}$  was optimized as  $0.125 \text{ s}^{-1}$ , leading to an equilibrium coefficient of 0.25. The rate coefficient for imine formation was obtained independently via following the imine yield under pseudo-first-order conditions in the absence of irradiation ( $k_{\text{imine}} = 0.20 \text{ L}\cdot\text{mol}^{-1}\cdot\text{s}^{-1}$ , Figure S17). Using 3.6 equiv of the amine in the absence of irradiation, the Diels–Alder product is not detectable when either 1.2 or 2.4 equiv of ethyl maleimide were employed, whereas the imine yield is 23% after 7 min. This imine yield of 23% is confirmed theoretically (first entry in Table 2). In this case, the system is thus not influenced by the initial amount of maleimide because the benzaldehyde is not photochemically transformed into the diene form. The rate coefficient for the photoinduced reaction with the maleimide ( $k_{\text{photo}}$ ) was set to  $50 \text{ L}\cdot\text{mol}^{-1}\cdot\text{s}^{-1}$  in order to achieve a good match with the experimental product yields at 7 min for different

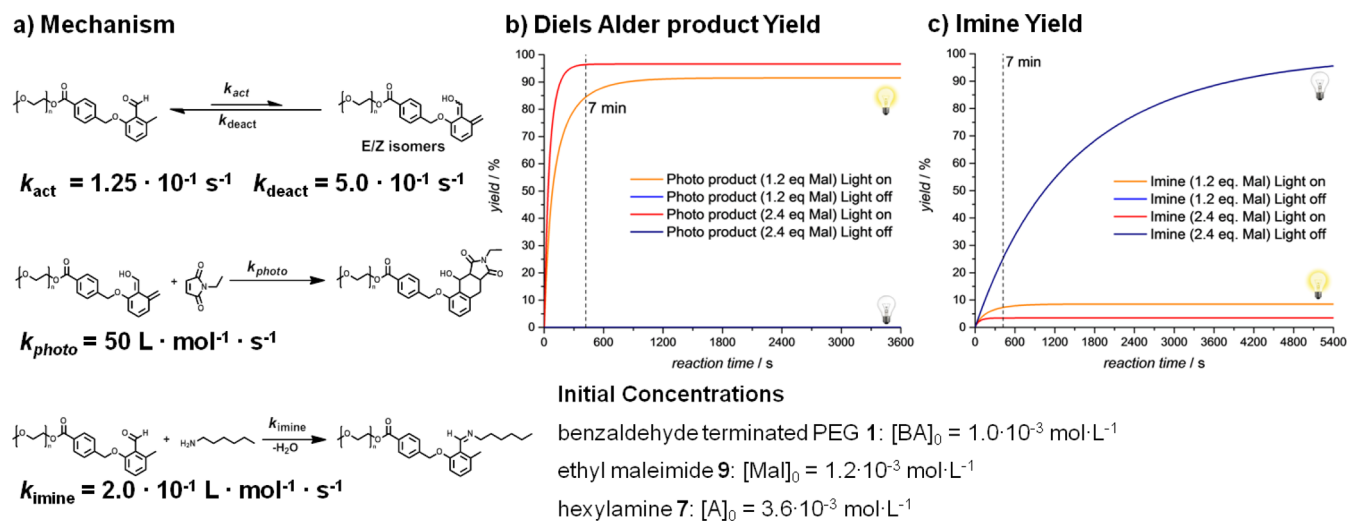


**Figure 2.** The mechanism of the proposed light-triggered reaction manifold is depicted including the assessed rate coefficients, using the experimental data in Table 2. The plots are simulated using the PREDICI software package. The reactions entail an equilibrium between *o*-methyl benzaldehyde PEG **1** and an in situ formed *o*-quinodimethane, the cycloaddition of the *o*-quinodimethane (the diene or photoenol) with ethyl maleimide **9**, and the imine formation based on the reaction of **1** with hexylamine **7**. An increasing maleimide initial concentration leads to a higher Diels–Alder yield with a simultaneous decrease of the imine yield during irradiation. Nonirradiative conditions trigger only the imine reaction because no diene (*o*-quinodimethane) is present.

**Table 2. Comparison of the Diels–Alder and Imine Yield Determined by Both Semiquantitative PREDICI Simulations and Experiments after a Reaction Time of 7 min, Additionally Simulated Nonconverted Fraction of the Benzaldehyde, and the Yield of the Photoenol (*o*-Quinodimethane)<sup>a</sup>**

maleimide amount (equiv)	PREDICI simulation				experiment	
	benzaldehyde	photoenol (diene)	Diels–Alder product	imine	Diels–Alder product	imine
0.0	75%	0%	0%	25%	0%	23 ± 2%
1.2	7%	1%	85%	7%	92 ± 2%	8 ± 2%
2.4	0%	0%	97%	3%	95 ± 2%	5 ± 2%

<sup>a</sup>MS-derived yields shown.

initial maleimide concentrations (refer to Table 2). For example, 1.2 equiv of **9** with 1.0 equiv of **1** and 3.6 equiv of **7** results in a simulated cycloadduct yield of 85% and an imine yield of 7% after 7 min with matching experimental data of 92 ± 2% and 8 ± 2%, respectively, based on the mass spectrometric analysis (Figure 3).

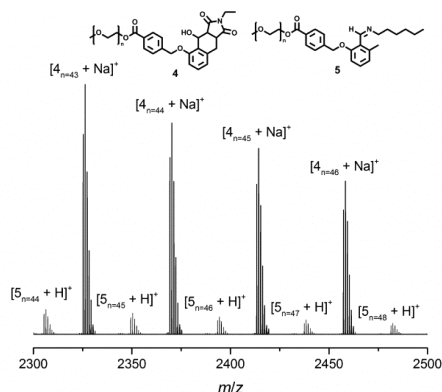


**Figure 3.** Mass spectrum of a system containing benzaldehyde-terminated PEG **1** (1.0 equiv), ethyl maleimide **9** (1.2 equiv), and hexylamine **7** (3.6 equiv) in dichloromethane. The system was irradiated for 7 min with a fluorescent PL-L lamp. Photo cycloadduct **4** and imine product **5** were detected via Orbitrap ESI-MS. The yield of the imine species is 8 ± 2%.

For comparison, <sup>1</sup>H NMR analysis reveals a very similar imine yield of 11 ± 2% (refer to Figure S22). An increase in the amount of **9** to 2.4 equiv (2.4 × 10<sup>-3</sup> mol·L<sup>-1</sup>) leads to a higher simulated yield of the cycloadduct (97%) and to a further decrease of the imine yield (3%) (refer to Figure 2b), again with matching experimental values of 95 ± 2% and 5 ± 2% (entry 3 in Table 2). For comparison, the imine yield determined via <sup>1</sup>H NMR is 7 ± 2% (refer to Figure S24). Thus, the maleimide acts as a diene trap. An increasing initial amount of maleimide shifts the equilibrium to the *o*-quinodimethane form of the benzaldehyde leading to the effective switch of the overall reaction to the Diels–Alder product formation. As explained in the Supporting Information, this observation also follows from a basic kinetic analysis, assuming for simplicity the quasi-steady-state approximation for the diene species and taking into account that simulations with the full kinetic model indicated a dominance for deactivation ( $k_{\text{deact}} \gg k_{\text{photo}} [\text{Mal}]_0$ ).

Next, we conduct a switching experiment based on the light-triggered reaction manifold concept. A mixture of benzaldehyde-terminated PEG **1**, ethyl maleimide **9**, and hexylamine **7** in dry dichloromethane was irradiated for 1 min at  $\lambda_{\text{max}} = 365$  nm and left subsequently for 5 min without irradiation. This on–off procedure was repeated three times with the overall results depicted in Figure 4.

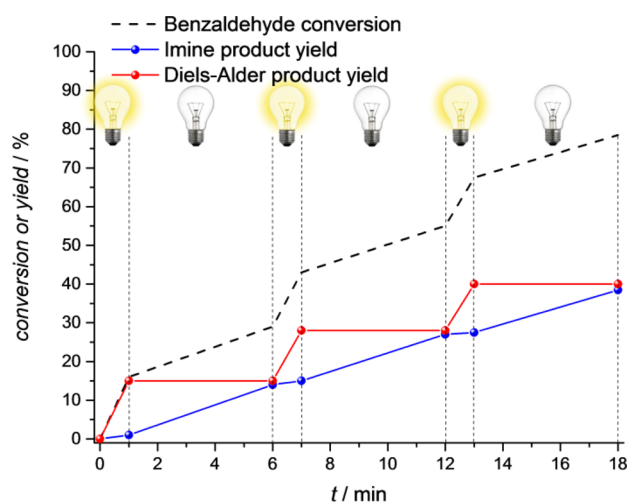


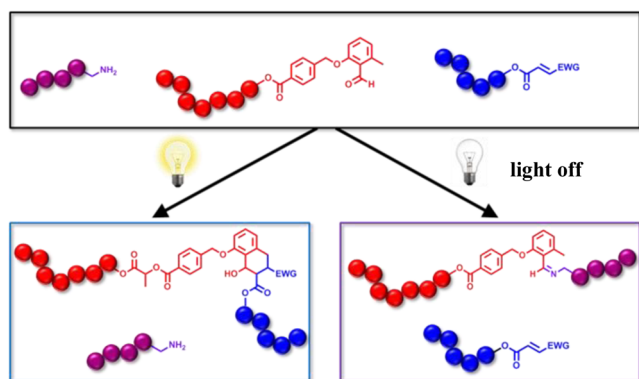
**Figure 4.** Switchable system containing 1.0 equiv of benzaldehyde-terminated PEG **1**, 1.2 equiv of ethyl maleimide **9**, and 3.6 equiv of hexylamine **7** was irradiated for 1 min and left nonirradiated for 5 min in an alternating fashion (three on–off cycles). The yield of the Diels–Alder product, the imine yield, and the benzaldehyde conversion were determined via high-resolution mass spectrometry; a linear interpolation was performed for simplicity.

The analysis requires an analytical method with a very short analysis time. Therefore, the yield of the Diels–Alder and the imine product in the switchable system were determined via high-resolution mass spectrometry (Orbitrap ESI-MS). The evolution of the photo product and the imine yield are depicted in Figure 4. The switchable system shows imine formation suppression in good agreement with the above experimental data during the irradiation procedure. Moreover, a linear extrapolation of the imine evolution during the irradiation periods up to 7 min in Figure 4 leads to a yield of close to 9% in excellent agreement with the second entry (experiment, 1.2 equiv of maleimide; Table 2). The thermal reaction is strongly suppressed during the light process and progresses only significantly in the dark time.

**Kinetic Preference of the Photoreaction over the Imine Formation.** The kinetics of the Diels–Alder reaction of the photochemically formed *o*-quinodimethane shows a highly solvent dependent effect, as noted above. The rate of product formation in a polar solvent such as acetonitrile is significantly faster than that in a nonprotic solvent such as dichloromethane used for evidencing the reaction manifold. Thus, the photoreaction rate in acetonitrile exceeds the imine formation rate substantially during the irradiation period. Therefore, the overall imine formation becomes negligible in the case where acetonitrile is used as solvent. The utilization of this purely kinetic variant of the reaction manifold can be exploited to design well-defined block copolymers from a one-pot system containing

a benzaldehyde terminal polymer, an amine-terminal polymer, and a maleimide terminal polymer. The requirements for the synthesis of pure block copolymers via modular ligation methods demand equimolar starting materials, quantitative conversions, and the absence of side reactions.<sup>29,39–41</sup> The selective block copolymer construction is triggered by either irradiating the one-pot system, leading to a fast photo adduct ligation of a benzaldehyde-capped polymer and an ene-capped polymer, or by nonirradiation of the one pot, resulting in the imine formation of a benzaldehyde-terminated polymer and the amine functionality. The concept is depicted in Scheme 3.

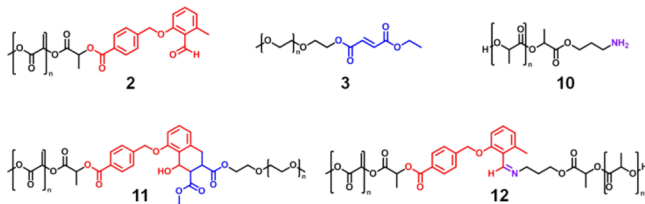
**Scheme 3. Orthogonal Construction of Block Copolymers by Applying the Kinetically Driven Version of the Reaction Manifold in a System Containing Benzaldehyde-Terminated Polymer, Ene-Terminated Polymer, and (Macromolecular) Amine Species<sup>a</sup>**



<sup>a</sup>The photoinduced and the nonirradiative reaction path lead to the selective formation of block copolymers.

All irradiations for the block copolymer synthesis were carried out with three high-power LEDs connected in series and emitting in the wavelength range between 350 and 400 nm ( $\lambda_{\max} = 375$  nm) in order to guarantee a more efficient irradiation leading to a fast photoreaction of the *o*-methyl benzaldehyde (refer to Figure S1). On the basis of the kinetic preference reaction manifold concept, two different one-pot systems are introduced for an orthogonal block copolymer synthesis (Scheme 4). Both systems represent an all polymer system including different polymer structures (i.e. poly(ethylene glycol), poly(L-lactide) and poly(*N*-isopropylacrylamide)). The first system contains *o*-methyl benzaldehyde capped poly(L-lactide) **2** (benzaldehyde-capped PL), fumarate-capped poly(ethylene glycol) **3** (PEG-fumarate),

**Scheme 4. Overview of Polymers That Are Employed for the Block Copolymer Synthesis in Acetonitrile<sup>a</sup>**



<sup>a</sup>Benzaldehyde-capped poly(L-lactide) (PL) **2**, fumarate-capped poly(ethylene glycol) (PEG) **3**, amine-capped poly(L-lactide) (PL) **10**, the Diels–Alder product PL-block-PEG **11** as well as the imine-linked PL-block-PL **12**.

and amine-capped poly(L-lactide) (PL-amine) **10**. The photo-reaction path was induced by irradiating a mixture of **2** with an equimolar amount of **3** and an equimolar amount of **10** in dry acetonitrile for 1 h with three LEDs. This ligation path led to the formation of PL-block-PEG **11** ( $M_n = 8200$  g·mol<sup>-1</sup>), whereas PL-amine **10** ( $M_n = 5000$  g·mol<sup>-1</sup>) remained unreacted. The polymers were analyzed via GPC (refer to Figure 5) and <sup>1</sup>H NMR (refer to Figure S32).

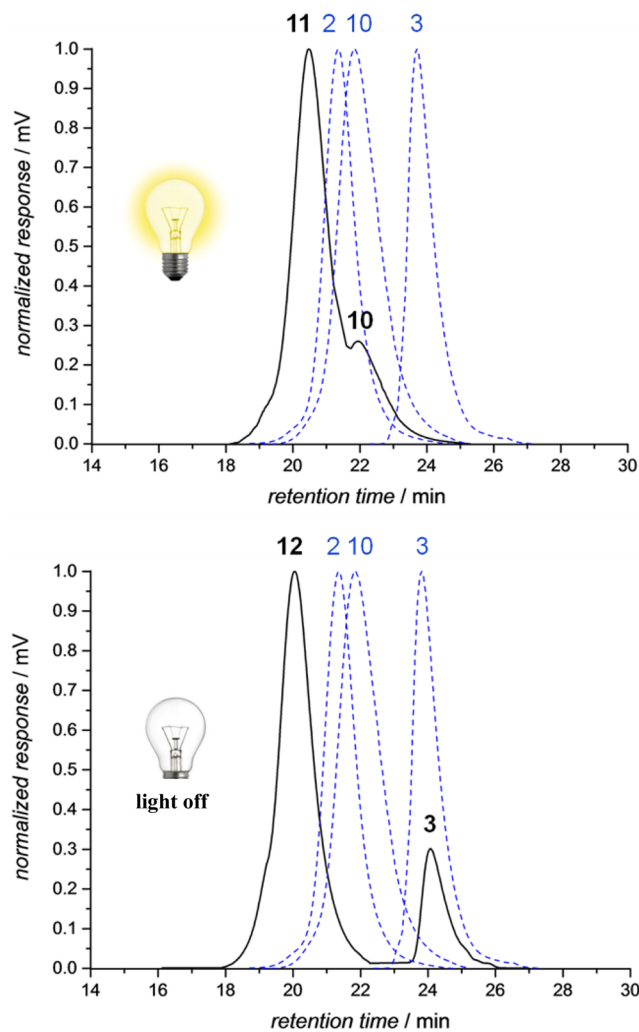


**Figure 5.** Benzaldehyde-terminated PL **2**, an equimolar amount of PEG-fumarate **3**, and an equimolar amount of PL-amine **10** in dry acetonitrile were irradiated for 1 h with three high-power LEDs, selectively forming PL-block-PEG **11** (top). The same system was stirred for 2 days at ambient temperature in dry acetonitrile, selectively forming PL-block-PL **12** (bottom).

Furthermore, the GPC traces were deconvoluted, and the resulting RI responses of the isolated signals were assigned to the sample weights of the starting polymers in order to evidence the orthogonal block copolymer formation (refer to Figure S34). The nonirradiative path was induced by stirring a mixture of **2** with an equimolar amount of **3** and an equimolar amount of PL-amine **10** in dry acetonitrile for 2 days in the dark. The imine path led to the formation of PL-block-PL ( $M_n = 11\,000$  g·mol<sup>-1</sup>) **12** and unreacted PEG-fumarate **3** ( $M_n = 2200$  g·mol<sup>-1</sup>) (refer to Figure 5). The success of the orthogonal block copolymer formation was evidenced via GPC (refer to Figure 5) and <sup>1</sup>H NMR (refer

Figure S35) including the calculated assignment of the weight of all starting materials similar to photoreaction path (refer to Figure S37).

To obtain the isolated GPC traces during the orthogonal block copolymer formation, the study was repeated by exchanging the macromolecular amine compound by a small amine functionality. This system contains *o*-methyl benzaldehyde capped poly(ethylene glycol) **1** (benzaldehyde-terminated PEG), maleimide-capped poly(*N*-isopropylacrylamide) **13** (pNI-PAAm-maleimide), and hexylamine **7** (refer to Figure S27). The GPC data of both systems reveal successful block copolymer formation indicated by a clear shift of the starting materials after either the irradiation with the LED or the nonirradiative ligation procedure of *o*-methyl benzaldehyde with amines.

## CONCLUSIONS

First, we introduce a novel *o*-methyl benzaldehyde reaction pathway with amines leading to imine formation. Second, we demonstrate that the nonirradiative transformation of the aldehyde moiety of the benzaldehyde with an amine functionality into an imine as well as the photoinduced click reaction between an *o*-quinodimethane (photogenerated diene species) and an activated ene functionality are the basis of an efficient light-triggered reaction manifold. The orthogonality of the reaction paths is achieved by the suppression of the imine formation by the photoreaction and the kinetic preference of the photoreaction over the thermal reaction. The first aspect featuring the suppression of the imine transformation is based on the photoinduced equilibrium between the benzaldehyde state and the *o*-quinodimethane (diene) state. The concept was underpinned by PREDICI simulations and was subsequently applied in a switchable end-group formation. The second aspect features the kinetic preference of the light-triggered reaction, constituting a tool for the selective synthesis of block copolymers. The present study shows that light-induced reactions can be employed to determine efficiently the propensity of thermal processes to occur, either by opening alternative reaction channels or by rate preference.

## ASSOCIATED CONTENT

### Supporting Information

The Supporting Information is available free of charge on the ACS Publications website at DOI: 10.1021/jacs.6b01805.

Full experimental details of all reaction manifolds including block copolymer syntheses. Emission spectra of the used light sources. UV/vis spectrum of the *o*-methyl benzaldehyde. <sup>1</sup>H NMR spectra of small molecule studies, polymers, and reaction manifold systems. ESI-MS spectra of polymers employed for the kinetic rate coefficient assessment within the reaction manifold systems. Kinetic assessment. GPC traces of polymers and proof of the orthogonal block copolymer formation. (PDF)

## AUTHOR INFORMATION

### Corresponding Authors

\*E-mail: christopher.barner-kowollik@kit.edu, christopher.barnerkowollik@qut.edu.au.

\*E-mail: j.blinco@qut.edu.au.

### Notes

The authors declare no competing financial interest.

## ACKNOWLEDGMENTS

C.B.-K. acknowledges funding from the Karlsruhe Institute of Technology (KIT) in the context of the Helmholtz STN program. K.H.'s Ph.D. studies are partly funded by the Fonds der Chemischen Industrie (FCI). Furthermore, C.B.-K. and J.B. acknowledge the DAAD/ATN for funding facilitating a visit of K.H. to the Queensland University of Technology (QUT). D.R.D. acknowledges the Fund for Scientific Research Flanders (FWO) for providing a postdoctoral fellowship.

## REFERENCES

- (1) Baskin, J. M.; Bertozzi, C. R. *QSAR Comb. Sci.* **2007**, *26*, 1211–1219.
- (2) Best, M. D. *Biochemistry* **2009**, *48*, 6571–6584.
- (3) Espeel, P.; Du Prez, F. E. *Macromolecules* **2015**, *48*, 2–14.
- (4) Bochet, C. G. *Angew. Chem., Int. Ed.* **2001**, *40*, 2071–2073.
- (5) Malkoch, M.; Thibault, R. J.; Drockenmuller, E.; Messerschmidt, M.; Voit, B.; Russell, T. P.; Hawker, C. J. *J. Am. Chem. Soc.* **2005**, *127*, 14942–14949.
- (6) Killops, K. L.; Campos, L. M.; Hawker, C. J. *J. Am. Chem. Soc.* **2008**, *130*, 5062–5064.
- (7) Camponovo, J.; Ruiz, J.; Cloutet, E.; Astruc, D. *Chem. - Eur. J.* **2009**, *15*, 2990–3002.
- (8) DeForest, C. A.; Polizzotti, B. D.; Anseth, K. S. *Nat. Mater.* **2009**, *8*, 659–664.
- (9) von Maltzahn, G.; Ren, Y.; Park, J.-H.; Min, D.-H.; Kotamraju, V. R.; Jayakumar, J.; Fogal, V.; Sailor, M. J.; Ruoslahti, E.; Bhatia, S. N. *Bioconjugate Chem.* **2008**, *19*, 1570–1578.
- (10) Poloukhine, A. A.; Mbua, N. E.; Wolfert, M. A.; Boons, G.-J.; Popik, V. V. *J. Am. Chem. Soc.* **2009**, *131*, 15769–15776.
- (11) Arumugam, S.; Orski, S. V.; Locklin, J.; Popik, V. V. *J. Am. Chem. Soc.* **2012**, *134*, 179–182.
- (12) Arumugam, S.; Popik, V. V. *J. Am. Chem. Soc.* **2012**, *134*, 8408–8411.
- (13) Delaittre, G.; Goldmann, A. S.; Mueller, J. O.; Barner-Kowollik, C. *Angew. Chem., Int. Ed.* **2015**, *54*, 11388–11403.
- (14) Matsuda, T.; Mizutani, M.; Arnold, S. C. *Macromolecules* **2000**, *33*, 795–800.
- (15) Kockler, K. B.; Haehnel, A. P.; Junkers, T.; Barner-Kowollik, C. *Macromol. Rapid Commun.* **2016**, *37*, 123–134.
- (16) Arnold, D. R.; Clarke, B. M., Jr. *Can. J. Chem.* **1975**, *53*, 1–11.
- (17) Oehlenschlaeger, K. K.; Mueller, J. O.; Heine, N. B.; Glassner, M.; Guimard, N. K.; Delaittre, G.; Schmidt, F. G.; Barner-Kowollik, C. *Angew. Chem., Int. Ed.* **2013**, *52*, 762–766.
- (18) Wilson, R. M.; Schnapp, K. A.; Patterson, W. S. *J. Am. Chem. Soc.* **1992**, *114*, 10987–10989.
- (19) Pauloehrl, T.; Delaittre, G.; Winkler, V.; Welle, A.; Bruns, M.; Börner, H. G.; Greiner, A. M.; Bastmeyer, M.; Barner-Kowollik, C. *Angew. Chem., Int. Ed.* **2012**, *51*, 1071–1074.
- (20) Haag, R.; Wirz, J.; Wagner, P. J. *Helv. Chim. Acta* **1977**, *60*, 2595–2607.
- (21) Small, R. D.; Scaiano, J. C. *J. Am. Chem. Soc.* **1977**, *99*, 7713–7714.
- (22) Gruending, T.; Oehlenschlaeger, K. K.; Frick, E.; Glassner, M.; Schmid, C.; Barner-Kowollik, C. *Macromol. Rapid Commun.* **2011**, *32*, 807–812.
- (23) Winkler, M.; Mueller, J. O.; Oehlenschlaeger, K. K.; Montero de Espinosa, L.; Meier, M. A. R.; Barner-Kowollik, C. *Macromolecules* **2012**, *45*, 5012–5019.
- (24) Tang, Q.; Wu, Y.; Sun, P.; Chen, Y.; Zhang, K. *Macromolecules* **2014**, *47*, 3775–3781.
- (25) Stolzer, L.; Ahmed, I.; Rodriguez-Emmenegger, C.; Trouillet, V.; Bockstaller, P.; Barner-Kowollik, C.; Fruk, L. *Chem. Commun.* **2014**, *50*, 4430–4433.
- (26) Glassner, M.; Oehlenschlaeger, K. K.; Welle, A.; Bruns, M.; Barner-Kowollik, C. *Chem. Commun.* **2013**, *49*, 633–635.

- (27) Richter, B.; Pauloehrl, T.; Kaschke, J.; Fichtner, D.; Fischer, J.; Greiner, A. M.; Wedlich, D.; Wegener, M.; Delaittre, G.; Barner-Kowollik, C.; Bastmeyer, M. *Adv. Mater.* **2013**, *25*, 6117–6122.
- (28) Hildebrandt, K.; Pauloehrl, T.; Blinco, J. P.; Linkert, K.; Börner, H. G.; Barner-Kowollik, C. *Angew. Chem., Int. Ed.* **2015**, *54*, 2838–2843.
- (29) Barner-Kowollik, C.; Du Prez, F. E.; Espeel, P.; Hawker, C. J.; Junkers, T.; Schlaad, H.; Van Camp, W. *Angew. Chem., Int. Ed.* **2011**, *50*, 60–62.
- (30) Kolb, H. C.; Finn, M. G.; Sharpless, K. B. *Angew. Chem., Int. Ed.* **2001**, *40*, 2004–2021.
- (31) Tron, G. C.; Piralì, T.; Billington, R. A.; Canonico, P. L.; Sorba, G.; Genazzani, A. A. *Med. Res. Rev.* **2008**, *28*, 278–308.
- (32) Redmond, R. W.; Scaiano, J. C. *J. Phys. Chem.* **1989**, *93*, 5347–5349.
- (33) Konosonoks, A.; Wright, P. J.; Tsao, M.-L.; Pika, J.; Novak, K.; Mandel, S. M.; Krause Bauer, J. A.; Bohne, C.; Gudmundsdóttir, A. D. *J. Org. Chem.* **2005**, *70*, 2763–2770.
- (34) Frick, E.; Schweigert, C.; Noble, B. B.; Ernst, H. A.; Lauer, A.; Liang, Y.; Voll, D.; Coote, M. L.; Unterreiner, A.-N.; Barner-Kowollik, C. *Macromolecules* **2016**, *49*, 80–89.
- (35) Huffman, K. R.; Loy, M.; Ullman, E. F. *J. Am. Chem. Soc.* **1965**, *87*, 5417–5423.
- (36) Porter, G.; Tchir, M. F. *J. Chem. Soc. D* **1970**, 1372–1373.
- (37) De Heer, J. *J. Chem. Educ.* **1957**, *34*, 375.
- (38) Quílez-Pardo, J.; Solaz-Portolés, J. J. *J. Res. Sci. Teach.* **1995**, *32*, 939–957.
- (39) Opsteen, J. A.; Van Hest, J. J. *Polym. Sci., Part A: Polym. Chem.* **2007**, *45*, 2913–2924.
- (40) Quémener, D.; Davis, T. P.; Barner-Kowollik, C.; Stenzel, M. H. *Chem. Commun.* **2006**, 5051–5053.
- (41) Zhang, M.; Rupa, P. A.; Feng, C.; Lin, K.; Lunn, D. J.; Oliver, A.; Nunns, A.; Whittell, G. R.; Manners, I.; Winnik, M. A. *Macromolecules* **2013**, *46*, 1296–1304.